Numerical simulation of Blade Vortex Interaction and Vortex Ring State aerodynamics using a fully time marching unsteady wake model

Benoit Rodriguez [1]

[1] Onera, 29 avenue Division Leclerc, BP72, F-92322 Châtillon Cedex, France
Tel: +33 1 46 73 42 64 - Fax: +33 1 46 73 41 46
e-mail: Benoit.Rodriguez@onera.fr

Key words: Free-wake, Blade Vortex Interaction, Vortex Ring State.

Abstract: The unsteady wake model MINT based on the Mudry's theory [1] describes the rigorous unsteady evolution of a wake modelized by a potential discontinuity surface. It has been already used for the simulation of helicopter in maneuvering flight conditions [2]. New improvements are implemented, which are validated for a Blade Vortex Interaction test case, the baseline test case of the HART I [3] wind tunnel campaign. This test case was chosen due to the accuracy of the wake computation needed to simulate the physics of the Blade Vortex Interaction phenomenon. The results obtained show a very good stability of the method and good agreement with the experimental results. This confirms the relevance of the MINT wake model to simulate this kind of phenomena where the main difficulty is an accurate simulation of the rotor wake. This good correlation encouraged us to use this tool for the simulation of the Vortex Ring State, a physical phenomenon characterized by a strong interaction between the rotor and its wake. The results of the simulated test case show trends qualitatively close to the experimental results [4].

NOMENCLATURE

C_zM^2	sectional thrust in the airfoil frame
r	spanwise location, m
R	blade radius, m
r_j	tip of blade segment i
Fz, Fy, Fx,	rotor loads, N
Vz	helicopter vertical speed, $m.s^{-1}$
Vh	helicopter advancing speed, $km.h^{-1}$
Γ_i	circulation of blade section i, s^{-1}
$\vec{\Phi}_i$	gradient of potential jump of panel i, $m^{-1}.s^{-1}$
Ψ	azimuth, deg
$\Delta\psi$	time step, deg

ABBREVIATIONS

BVI	Blade Vortex Interaction
VRS	Vortex Ring State

INTRODUCTION

A better integration of helicopters in an urban area will need a reduction of the noise radiated. In approach flight, the Blade Vortex Interaction is the main noise source. In order to reduce it, research studies have been undertaken along several directions.

A first one is the better understanding of the BVI thanks to experimental campaigns such as the HART wind tunnel campaigns [3]. A second area of research is the development of numerical method dedicated to the BVI predictions. CFD methods developed for rotorcraft are evaluated on this configuration, but currently, the BVI is quite difficult to compute due to the diffusion of the tip vortex from the emission to the interaction. Using very fine meshes and high order schemes allows to capture some blade vortex interactions [5], but the CPU requirements are huge and the interactions are not well predicted. Despite the limitation of the modelization used in free-wake models, they allow maintaining the vortex properties without diffusion with much less CPU requirements than CFD methods. Nevertheless, these free-wake methods have to be stable enough to allow a reduction of the computational time step to simulate the blade vortex interaction, which is not so easy. Currently, the MESIR free-wake model used in the computation chain for BVI noise prediction only provides the wake geometry without being able to compute the oscillation of the sectional loads due to the BVI [6]. A third area of research related to the BVI is the study of flight maneuvers which could reduce the noise radiated [7]. But these maneuvering flights are limited by safety reasons for the helicopter flight limit in descent. The Vortex Ring State is the first limiting regime in steep descent. Flight tests campaign [8] and numerical studies [9][10][11] have been achieved to investigate the VRS.

The interest of having in hand a tool able to predict the aerodynamic loads of a helicopter in BVI or VRS with a reasonable CPU time requirement is undeniable.

The first part of the paper presents improvements in the discretization of the wake in the MINT code. This new version of the time marching free-wake model MINT is evaluated for a classical BVI test case and also several flight conditions of VRS entry. The interest of using the MINT code for such configurations will be pointed out and show the efficiency of MINT to simulate such kind phenomena.

1. UNSTEADY WAKE MODEL

1.1 The MINT Code

The wake model MINT was developed at ONERA [2] to get an efficient and accurate tool to compute the unsteady wake of helicopter rotor starting from both the METAR prescribed wake and MESIR free-wake models of ONERA and EUROCOPTER. For the blade aerodynamics, an unsteady lifting line theory is used with the computation of the aerodynamic airloads thanks to experimental airfoils tables. The innovative aspect of the code is the wake modelization. It is based on the Mudry theory [1], which details rigorously the unsteady evolution of a wake modelized by a potential discontinuity surface. The wake (see Figure 7) itself is discretized in panels of constant gradient of potential jump. This discretization improves the order of accuracy and the stability of the method compared to the discretization of the wake by lattices. The numerical integration used to compute the velocities induced by the panels is performed with a 4 points Gauss method [2]. The time marching scheme is a one step Runge-Kutta scheme with sub-iterations to converge the circulation on the blade and the emission condition of the wake at each time step.

1.2 New Improvements

1.2.1 Circulation at the blade tip

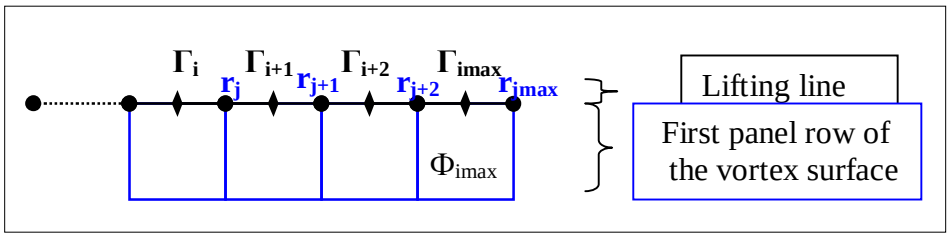

Figure 1: Discretization of the lifting line and the wake (first row of panels)

The initial discretization of the lifting line and the first row of panels of the wake is presented in Figure 1. The circulation Γ_i at the middle of each segment of the lifting line is estimated using the unsteady lifting line theory and the airfoils tables. To compute the gradient of potential jump on each panel, the value of the circulation is needed at each edge tip r_j of the lifting line segment. This value is obtained by a first order centered scheme. At the blade root and tip, the value of the circulation is extrapolated and not imposed to zero. Due to the theory, in case of a circulation value not equal to zero at these locations, a vortex line of intensity equal to the root and tip circulation is emitted in the wake. If the root and tip circulation is left free, then the circulation in the blade section located in the vicinity of these points may be far from the expected value. Moreover, the lattices introduce higher-order singularities in the computation which reduce the stability.

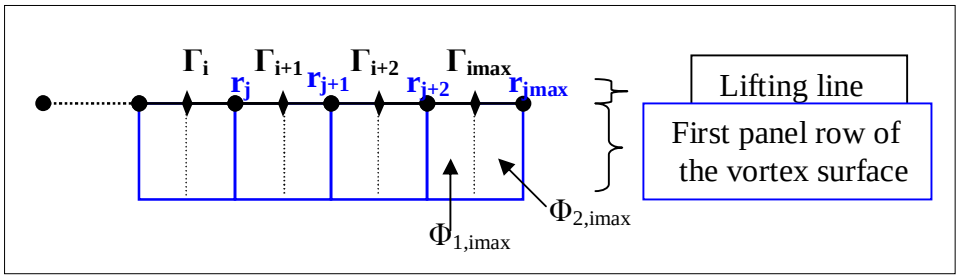

Figure 2: New discretization of the panels of the wake (first row of panels)

A solution considered is to impose as a boundary condition the physical value of zero to the circulation at the blade tip and root. However the circulation obtained along the blade with this correction is very oscillating. In fact due to the modelization presented in Figure 1, oscillating values of circulation can be computed at the middle of the blade segment without changing the value of the circulation at the panels' vertices and so without changing the gradient of potential on the panels: the computation is not stable. A way to correct this phenomenon is to take into account the value at the middle of the lifting line section in the computation of the gradient of potential jump on the panel. Figure 2 presents the new discretization of the first row of panels of the wake. This new discretization allows to suppress the oscillations due to an imposed value of circulation equal to zero at the blade tips.

An additional interest of this discretization is that, with a value of circulation equal to zero at the blade root and tip, there is no more need for the lattices at the wake borders and the discretization of the gradient of potential jump is more accurate. However, numerical test show that the improvements are only noticeable with small time steps. It was necessary to find a solution for larger time steps.

1.2.2 Numerical computation of panel at the first row on the blade

At each time step a new row of panels is emitted by the blade. The aspect ratio of the panel is therefore related to the time step. With large time steps, the aspect ratio of the panels is very large

especially at the blade tip where the blade velocity is the highest. This increases the numerical error of the integration to compute the velocity induced by the panels. To improve the integration, panels of high aspect ratio are converted into a subgroup of smaller panels with a convenient aspect ratio. This technique allows to improve the numerical integration for large time steps.

With these improvements the computed circulation on the blade and the gradients of potential jump on the panels are more accurate at the blade tip especially with the fairly coarse discretizations used to solve the problem. The wake modelization is better especially the modelization of the tip vortex. Moreover from a numerical point of view, the suppression of the vortex lattices at the edges of the wake removes all higher-order singularities. All these considerations are important for the cases which will be computed when the rotor interacts directly with the wake.

1.3 Computation procedure

The computation of a test case with MINT needs to prescribe the rotor controls and dynamics (rigid or soft blade) as input. The data is obtained from the comprehensive dynamic code HOST [12] developed by Eurocopter. Typically MINT requires 20 hours of CPU time on a NEC SX8 to compute three rotor revolutions with a time step equivalent to 2°.

2. BLADE VORTEX INTERACTION

2.1 Test case

The test case considered is the HART I Baseline test case [3]. The rotor is a fully instrumented Bo-105 model rotor in descent flight. The shaft angle is equal to α_q=4.2° with an advance ratio of μ=0.15.

2.2 Results

Four computations of the test case were performed with the same inputs but with different time steps, starting from a time step equivalent to 10° of azimuth down to a time step equivalent to 1°. Figure 3 shows the sectional loads obtained for each computation at different spanwise locations compared to the experimental results. All computations provide good agreement with the experimental results as far as the low frequency component of lift is concerned. This is more particularly the case at r/R=0.97 which confirms the relevance of the improvements detailed in 1.2. Figure 4 presents a close view of the sectional loads for the advancing blade side. With a reduce time step, the oscillations typical of the BVI appear. The same phenomenon is obtained for the retreating blade (see Figure 5). These oscillations appear gradually with the time step reduction which allows to improve the temporal accuracy of the computation but also the spatial accuracy due to a reduction of the panel size discretizing the wake (a new row of panels is emitted at each time step). The computed BVI oscillations are in good agreement with experiment and it can be seen that no new oscillation is created. This gives an indication that MINT converges toward the capture of the BVI events.
The Blade Vortex Interaction is a very impulsive phenomenon. As shown above, it is necessary to reduce the time step to see the appearance of the sectional loads oscillations due to BVI. A way to qualify the quality of the computation is to compare the derivate of the computational sectional loads to the experimental ones (see Figure 6). The derivative of the sectional load at r/R=0.75 for the computation with a time step equivalent to 1° is compared with the experimental results. The computation is very close to the experiment, with derivatives of the sectional loads well predicted. However a slight phase lag is present and some interactions are missing. It is expected to improve

these results with a weak coupling between the HOST code and the MINT code which could modify slightly the blade dynamics and trim and so the times and positions of the blade vortex interactions.

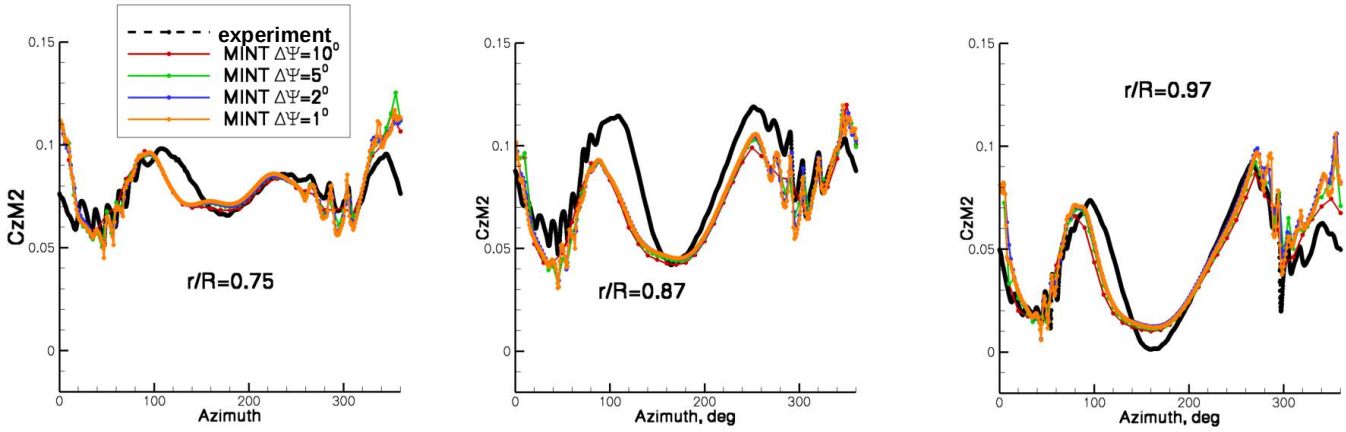

Figure 3: Sectional loads at several spanwise locations for several time step scales

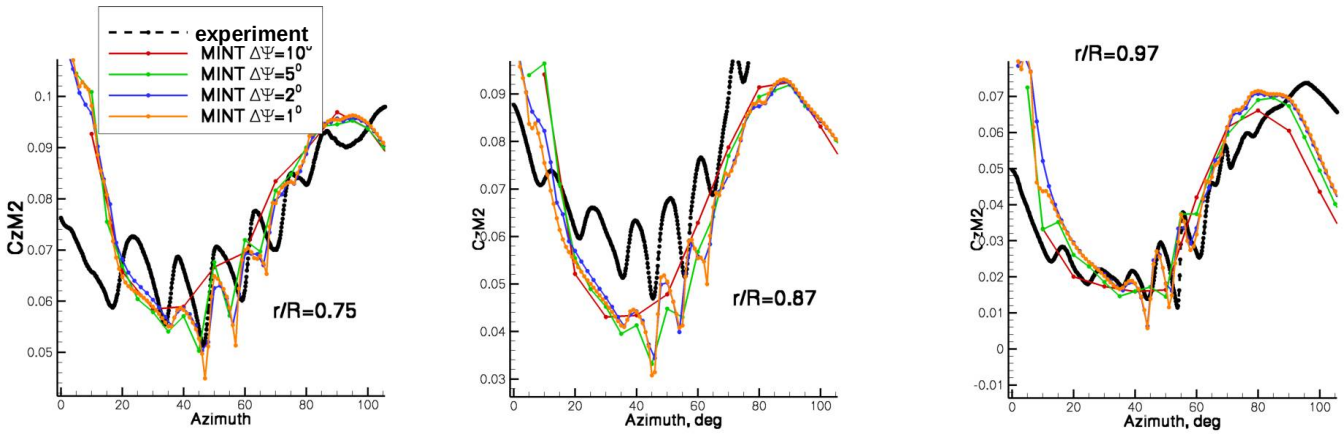

Figure 4: Sectional loads at three spanwise locations for four time step scales for the advancing blade

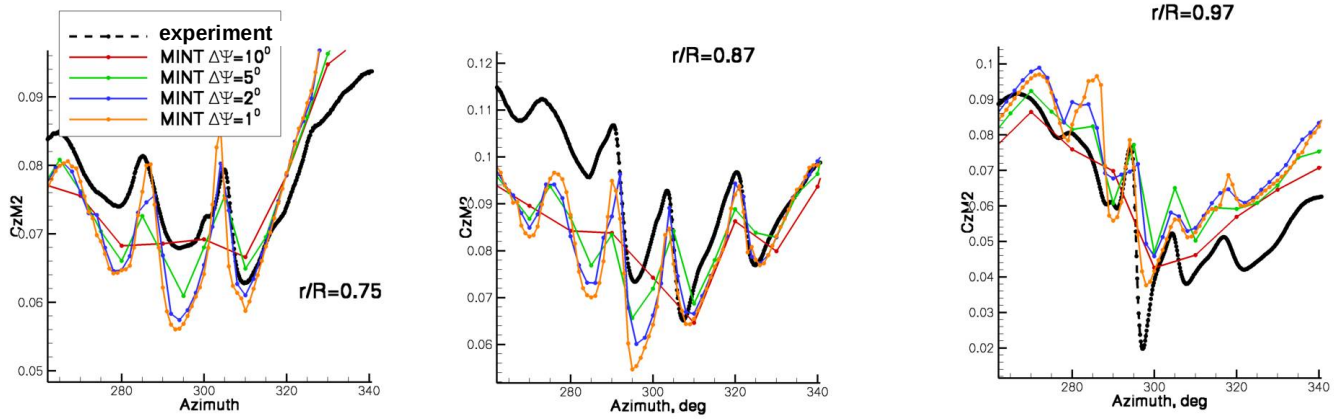

Figure 5: Sectional loads at three spanwise locations for four time step scales for the retreating blade

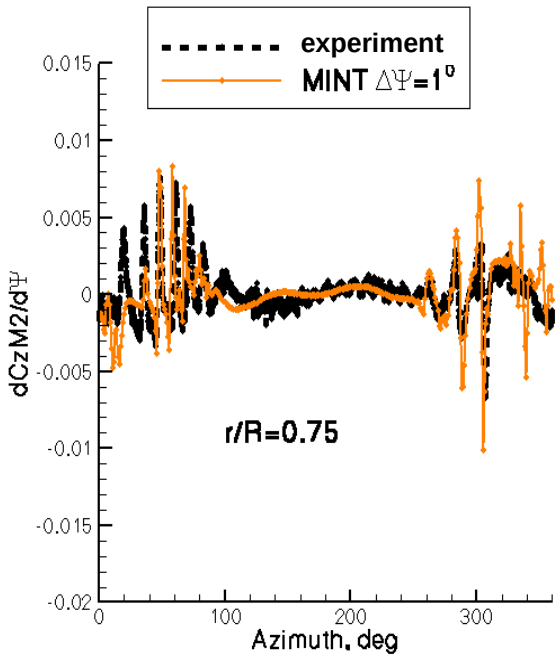

Figure 6: Derivative of the sectional loads at r/R=0.75 and with Δψ=1°

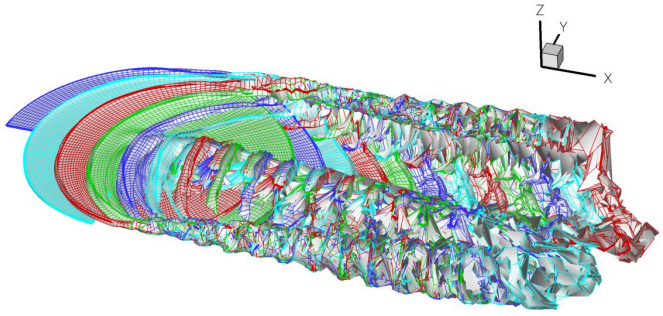

Figure 7: MINT wake of the baseline test case of HART I

3. VORTEX RING STATE

3.1 Test case

In cooperation with the French flight test center CEV, ONERA performed an experimental and theoretical study on VRS. It goal was the development of an aerodynamic model of the rotor in steep descent. Reference [5] details the results of this study. The Dauphin 6075 helicopter was used to realize the flight tests, of which some results are presented in Figure 8. To compare our results to with the experimental one, it was decided to simulate a Dauphin 365N, configuration close to the experimental one.

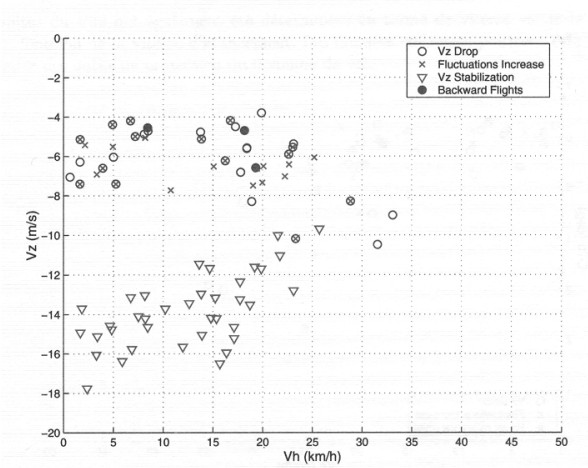

Figure 8: D6075 VRS boundaries plotted in (Vz,Vh) diagram (from [5])

Two advancing velocities were chosen for the flight conditions studied in the present paper. The first one corresponds to a velocity of VH=0km/s. For the second one, the velocity is VH=15km/h, corresponding to a configuration located in the middle of the VRS domain (Figure 8).

3.2 Computation strategy

The comprehensive dynamic code HOST provided the helicopter dynamics (the trim: collective pitch, cyclic pitch, flap and the attitude) considering a stabilized flight based on an induced velocities model in steep descent [6]. In the present study, the blades are considered rigid in order to simplify the computations and the HOST trim is prescribed.
In Figure 9, the collective pitch (computed by HOST) is plotted for stabilized flights at different descent velocities for an advancing velocity equal to zero. For the descent velocities before the VRS regime, the collective pitch decreases with the velocity because of the increase of the blade angle of attack by the composition of the rotor rotation speed and the descent velocity of the helicopter. Figure 9 also shows the same results for an advancing velocity equal to 15km/h where VRS also appears. The VRS regime appears clearly with the loss of efficiency of the rotor which requires an increase of the collective pitch to stabilize the helicopter despite the decrease of the descent velocity.

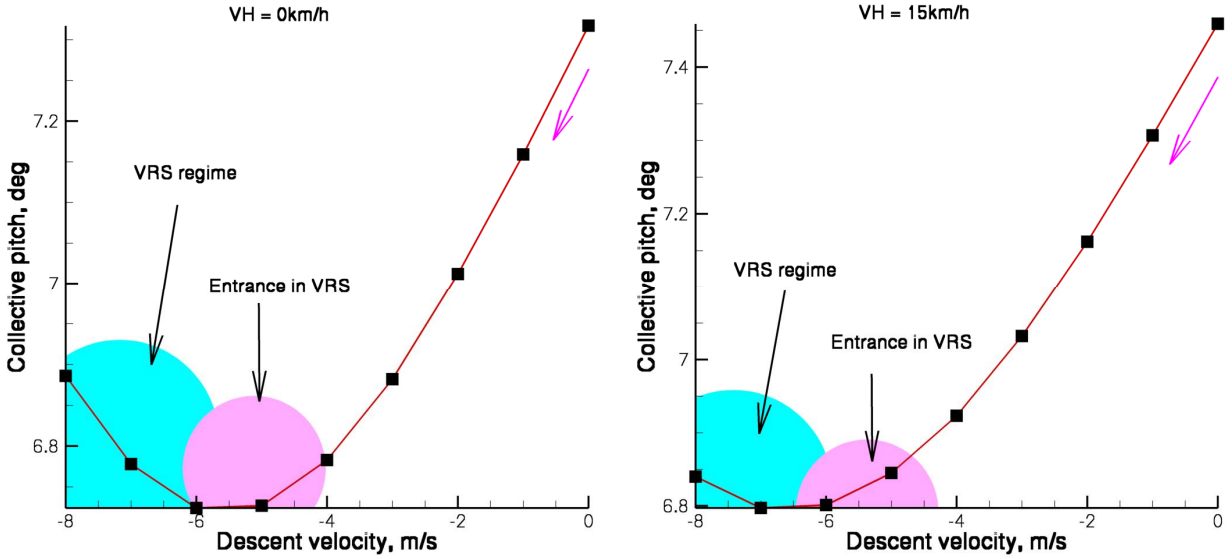

Figure 9: Collective pitch computed by the HOST code for stabilized flights at different descent velocities with an advancing velocity equal to 0km/h or 15km/h

For each advancing velocity, a parametric study was performed with the MINT code by varying the vertical velocity from VZ=0m/s to VZ=-6m/s, with an entry in the VRS domain around VZ=-5m/s. The computations performed with MINT correspond to a succession of stabilized flights. Figure 10 presents the descending velocity depending on the number of rotor revolutions computed with the MINT code. For each simulation, the corresponding collective pitch can be found in Figure 9.

The blade is discretized by 25 sections in the spanwise direction. The time step is equivalent to 5° and a one-step Runge-Kutta scheme is applied in advance in time.

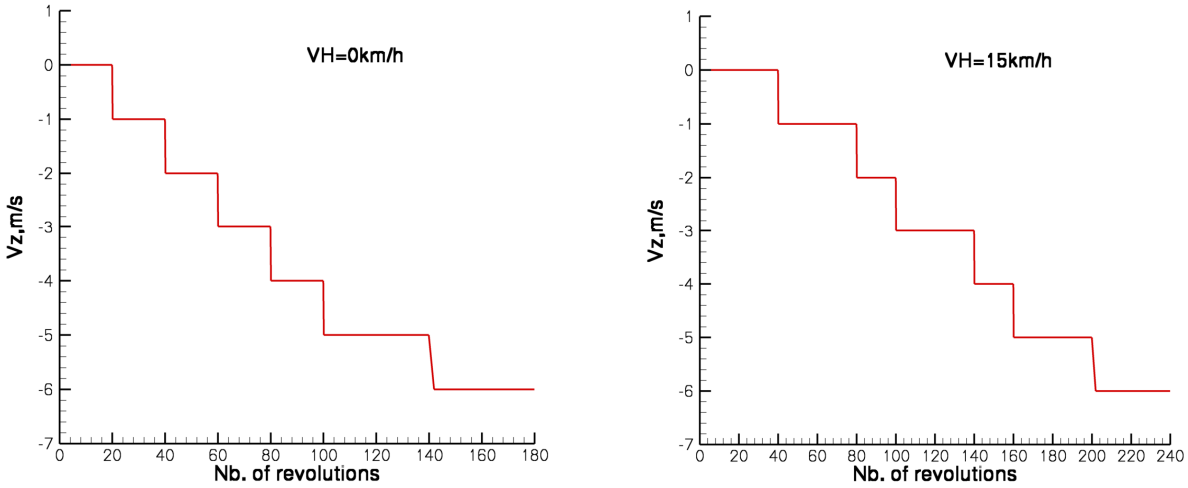

Figure 10: Descending speed depending on the number of rotor revolutions computed by the MINT code

3.3 Results in axial flight, VH=0m/s

3.3.1 Rotor loads

Figure 11 shows the evolution of the rotor thrust all along the computation. Each time the descending velocity is changed, a transient phase appears. The mean value of the thrust computed with MINT is slightly lower than the one computed by HOST which is necessary to have a stabilized flight. This mean value also decreases with the iterations. The difference between the thrust estimated by HOST and by MINT is due to the different aerodynamic models in the two codes. This could be improved by correcting the dynamics imposed to MINT, for example by coupling MINT and HOST. Such a coupling was not performed in the present study but can be envisaged in the future. As a result of these differences in the thrust, an entry in the VRS regime is expected slightly earlier in the MINT computations than in the HOST code.

The computed thrust is really noisy but one can notice a change in the signal for high descending velocities. At VZ=-5m/s (close to the entry in VRS in the experiments Figure 8), a low frequency oscillation seems to appear, and the amplitude of the thrust oscillations increases significantly. A frequency-time post-processing was applied to the thrust signal, consisting of a short Fourier transform of the thrust applied through a numerical window (Hamming) moving with time (TFFG). It allows the study of the evolution of the spectrum of the thrust with time. Figure 12 presents the results obtained. It confirms that when the descending velocity becomes equal to -5m/s low-frequencies appear in the thrust time evolution. An accurate computation of the value of the frequency of these oscillations is difficult to obtain due to the limited number of computed rotor revolutions but it is around $\Omega/10$. Figure 12 also shows the appearance of oscillations with a frequency equal to a multiple of the blade passage (4Ω, 8Ω, 16Ω).

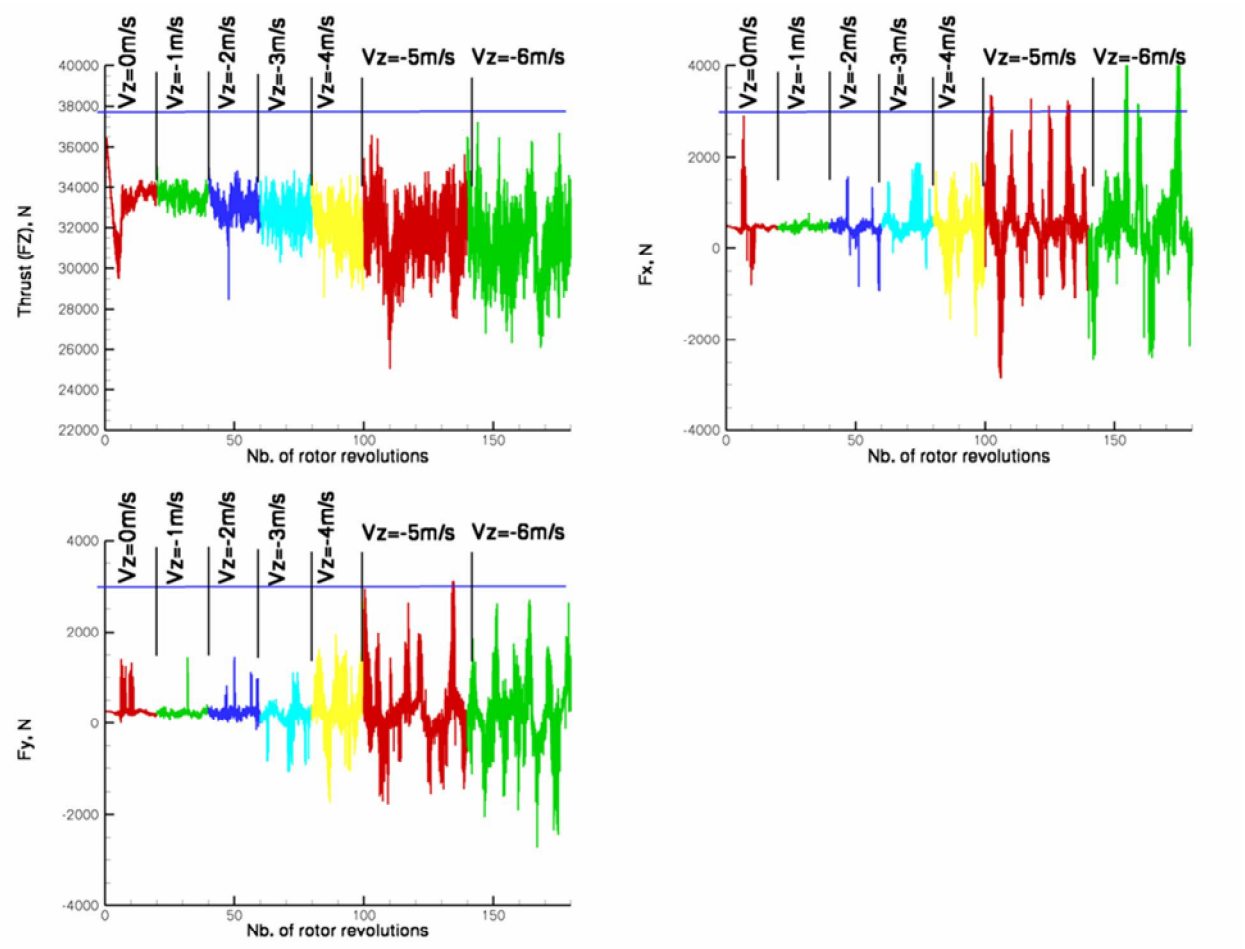

Figure 11: Evolution of the rotor loads with the descending velocity at VH=0km/h

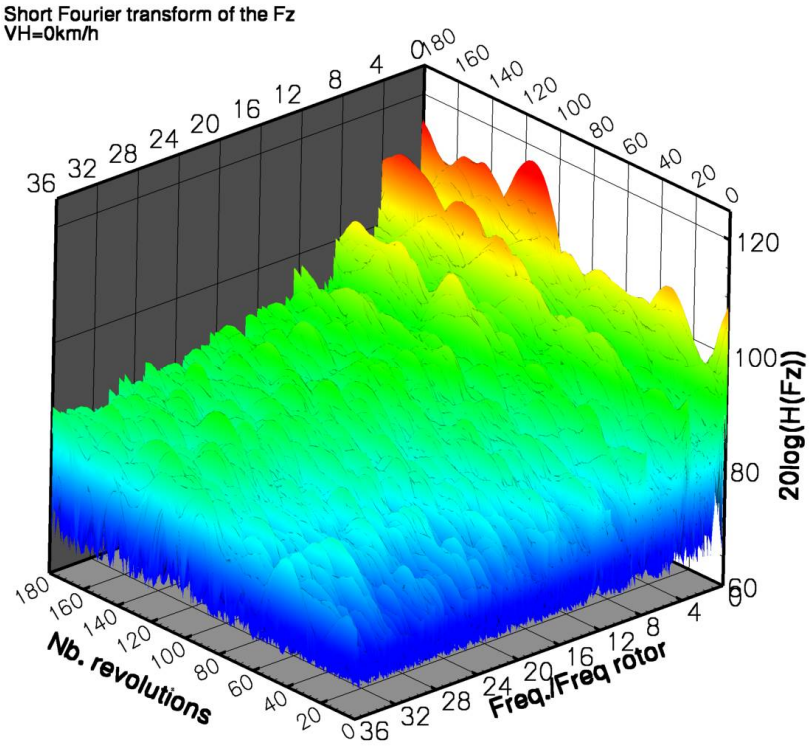

Figure 12: Frequency-time post-processing with a Fourier transform of the thrust at VH=0km/h

3.3.2 Beginning of the VRS regime

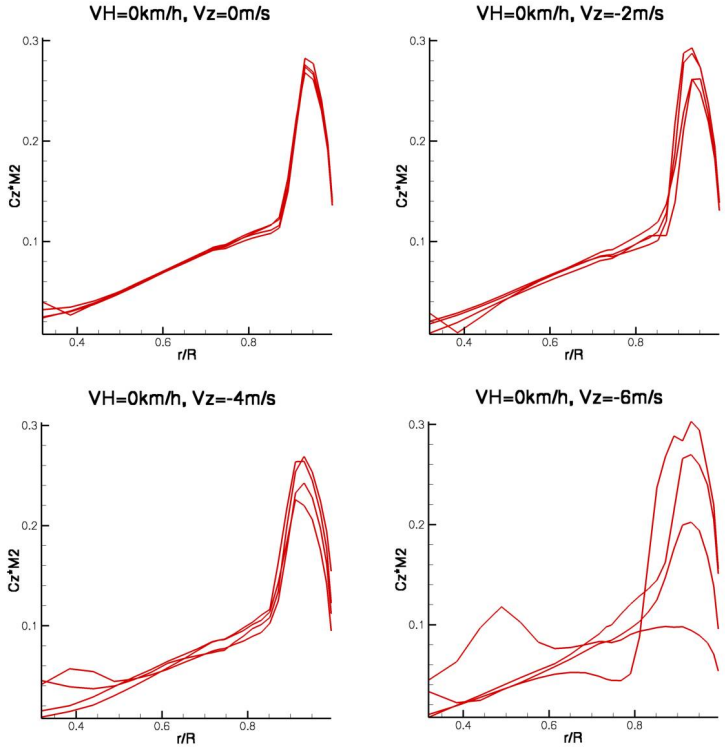

Figure 13: Evolution of the sectional loads along the spanwise direction with the descending velocity (4 azimuths of a blade rotation)

Figure 13 shows the sectional loads of a blade for different azimuths during one revolution for different descending speed values. It can be checked that the CzM2 values are quite steady for a descending velocity equal to 0/-2/-4 m/s. The only unsteadiness is mainly due to the cyclic commands applied from the HOST trim. On the contrary at -6m/s (considered as the entry in VRS) the evolution of the CzM2 is not at all steady. There are big variations during one revolution especially at the blade tip and for one plotted azimuth at r/R=0.45. These results explain the 4Ω and 8Ω frequencies appearing on the thrust at the VRS entry. To better understand the reason of such loads oscillations, a study of the wake is necessary.

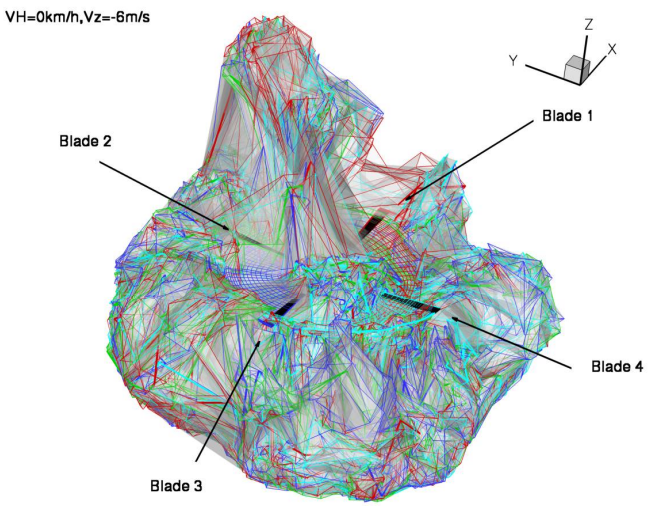

Figure 14: Vortex surfaces computed in the MINT code, model of the wake of the rotor

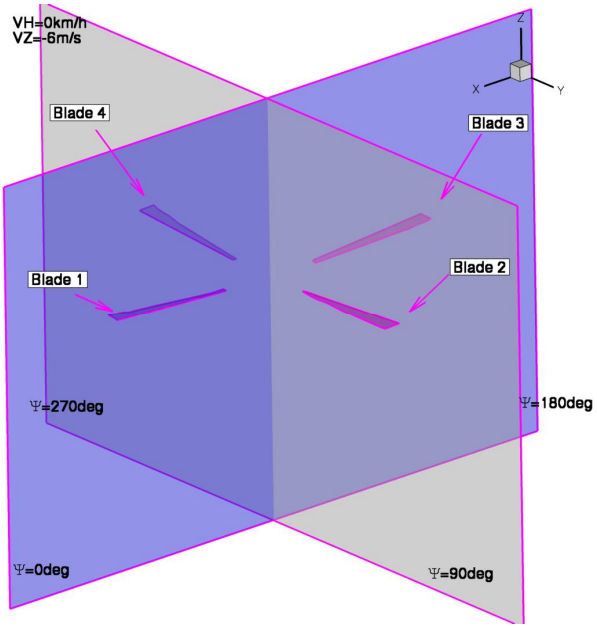

Figure 15: View of the slices used to present the velocities in the field

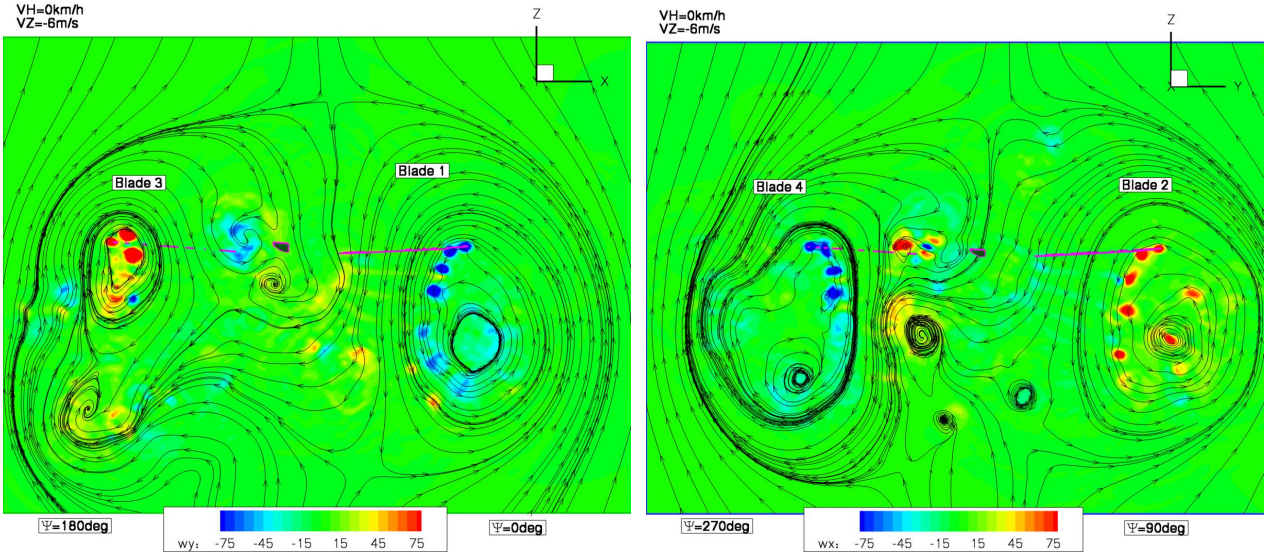

Figure 16: Slices XZ and YZ with the streamlines and the normal vorticity plotted

Figure 14 presents the wake sheets computed in the MINT code at the final time step of the computation performed at Vh=0km/h and Vz=-6m/s. It can be seen that the vortex surface is very close to the blade. It seems that a part of the wake is evacuated above the rotor. With this representation, it is very difficult to understand the flow physics, the velocity field was computed in a box surrounding the rotor. In this field, two slices were therefore post-processed and are presented in Figure 15.

Figure 16, the contours of normal vorticity and the streamlines in these two slices are plotted. In this figure, it can be seen that the position of the recirculation relative to the blade is different for each blade. These different positions induce different positions of the tip vortex with respect to the blade. For blade 1, the recirculation is below the blade and the tip vortex of the preceding blade is below the blade but quite close. For blade 3, the recirculation at the level of the rotor plane induces a

position of the tip vortex of the preceding blade above the current blade. For blade 2, the recirculation is far below the blade and the vortex of the preceding blade is also below the blade. For blade 4, two recirculations appear: one is close to the blade and the other one is far below. For blade 4, the tip vortex of the preceding blade is slightly above the blade and creates the small recirculation close to the blade. A group of vortices is also present at the blade root of blade 4.

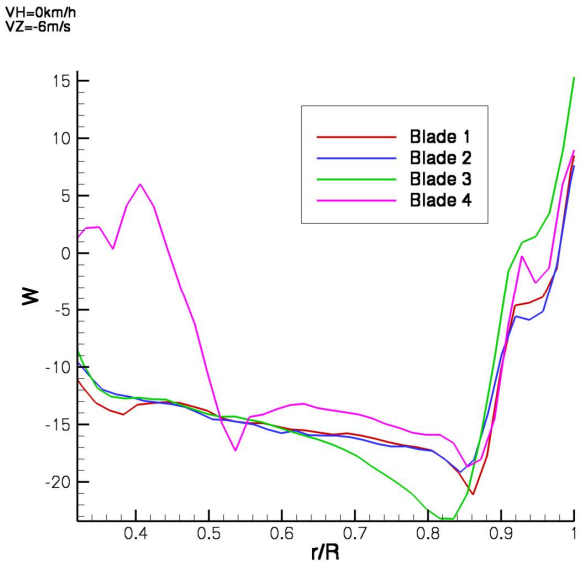

Figure 17: Vertical flow velocity at the blades position

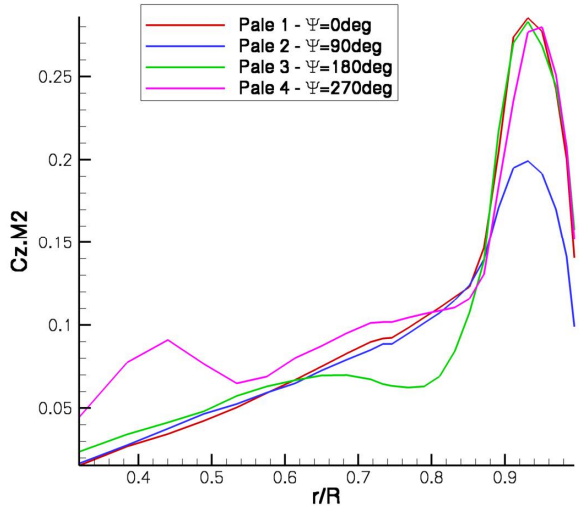

Figure 18: Sectional loads along the spanwise direction corresponding to the blades in Figure 16

The position of the vortices induces modifications of the velocity and especially of its component which mainly changes the angle of attack of the blade. In Figure 17, the evolution of the vertical velocity component is plotted along the 4 blades corresponding to the slices of Figure 16. The sectional loads along the spanwise direction of the 4 blades are shown in Figure 18. They are mainly correlated to the vertical component of inflow. The peaks and the levels of the loads are quite well correlated to the vertical velocity. For example, the peak of load at the blade root of blade 4 is linked to the vertical velocity disturbance at the same location.

The Fourier transform of the sectional load of the blade at r/R=0.93 (position of the peak) was performed for VH=0km/h and VZ=-6m/s. The main modes 1Ω, 2Ω, 3Ω were easily identified. With the four blades, these modes produce the 4Ω, 8Ω, 12Ω modes of the rotor thrust. The low-frequency mode of the thrust also appears in the spectrum of the sectional loads around Ω/10.

3.4 Results in advancing flight

As for the case in axial flight, big loads oscillations appear at VZ=-5m/s which characterize the entry in the VRS regime (see Figure 8).

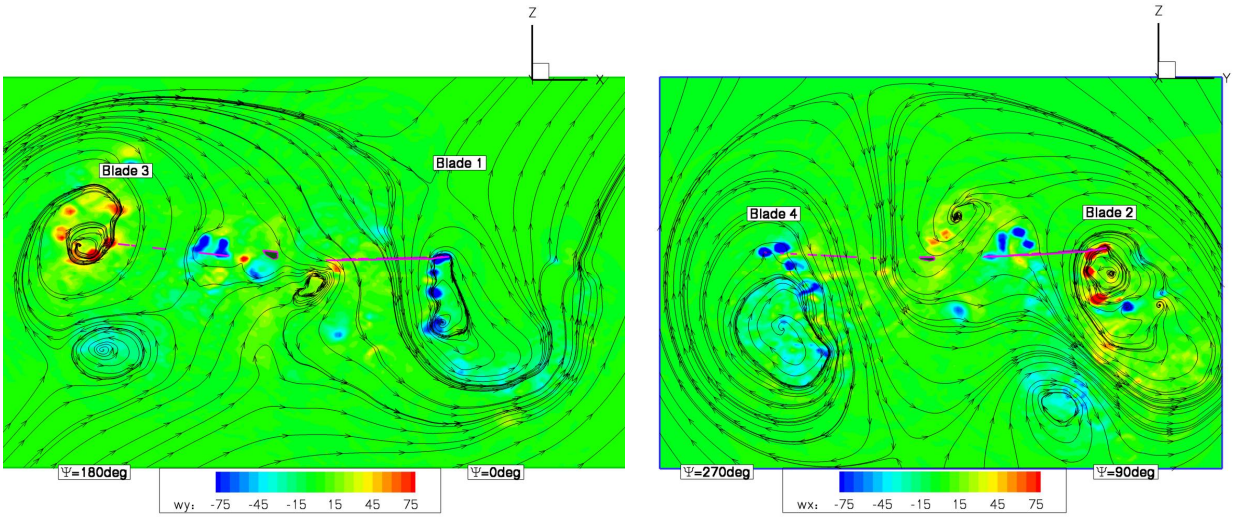

Figure 19: Slices XZ and YZ, with the streamlines and the normal vorticity plotted at VH=15km/h and VZ=-6m/s

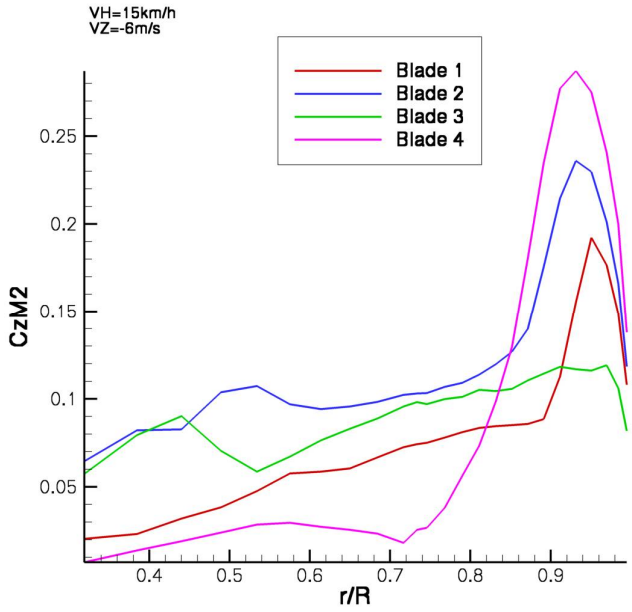

Figure 20: Sectional loads of the blades plotted in Figure 19

Two slices of the velocity field at VZ=-6m/s are plotted in Figure 19. The slice XZ is parallel to the advancing velocity VH. Big differences can be seen between the forward blade (blade 3) and the aft blade (blade 1). For blade 3, the convection is close to the blade and at the level of the rotor disk. One can clearly see the recirculation of the tip vortices from below to above the blade. For blade 1, the recirculation has a larger extent and the tip vortices do not come back from below the blade. In the slice YZ, the recirculations are almost symmetric but with a recirculation closer to blade 2 (advancing side) than to blade 4 (retreating side), However, the tip vortex is located just below blade 2 and above blade 4.

The sectional loads of the four blades are plotted in Figure 20. The peak of loads at the blade tip is clearly correlated to the position of the tip vortex of the preceding blade. In the case of blade 3, this peak disappears because the tip vortex of the preceding blade is not located below the blade but more outboard.

The wake geometry and the position of the recirculation are thus modified by the advancing velocity compared to the case at VH=0km/h. The flowfield and the blades loads are clearly impacted by this forward velocity.

CONCLUSION

Several developments were implemented in the MINT code to improve its accuracy and stability. They have been tested for the BVI test case of the HART I wind tunnel campaign. The results obtained are stable and in a good agreement with the experimental results, especially the high frequency oscillation of the sectional loads characteristics of the BVI phenomenon. The computation of the radiated noise from these wake predictions will be considered in the near future. Moreover new developments for the lifting line theory will also be implemented to improve the method [14].

In the second part of the study, the VRS has been investigated for a flight test configuration of the Dauphin 6075. The results show a good agreement with the experiment for the limit speed of VRS entry. The analysis of the results show that the VRS seems to be due to the interaction between the blade and a grouping of the tip vortices closer to the blade with the increased descend speed. It could be interesting to purse the study for other advancing speeds and for a complete simulation of VRS entry.

ACKNOWLEDGMENTS

The author would like to acknowledge the French Ministry of Transport (DPAC) to financially support a part of this study and his colleagues for the technical exchanges during this study and the writing of this paper.

REFERENCES

[1] M. Mudry, *"La théorie des nappes tourbillonnaires et ses applications à l'aérodynamique instationnaire"*, Thèse de Doctorat d'Etat, Univ. Paris VI, July 1982.

[2] G. Lebouar, M. Costes, A. Leroy-Chesneau, P. Devinant, "*Numerical simulations of unsteady aerodynamics of helicopter rotor in maneuvering flight conditions*", Aerospace Science and Technology, vol. 8, pp. 11-25, 2004.

[3] R. Kube et al, *"Initial Results from the Higher Harmonic Control Aeroacoustic Rotor Test (HART) in the German-Dutch Wind-tunnel"*, 75th AGARD Fluid Dynamic Panel Meeting on Aerodynamics and Aeroacoustics of Rotorcraft, Berlin, October 1994

[4] R. S. Bramwell, *"Helicopter Dynamics"*, Editions Edwards Arnolds, pp 85-86, 1976

[5] M. Dietz, E. Krämer, S. Wagner, *"Tip vortex conservation on a main rotor in slow descent flight using vortex adapted chimera grid"*, 24th AIAA Applied Aerodynamics Conference, San Francisco, USA, 5-8 June, 2006

[6] P. Beaumier, Y. Delrieux, "*Description and validation of the ONERA computational method for the prediction of the blade-vortex interaction noise*", Aerospace Science and Technology 9, pp. 31-43, 2005

[7] G. Perez, M. Costes, "*A new aerodynamic &acoustic computation chain for BVI noise prediction in unsteady flight conditions*", 60th American Helicopter Society Annual Forum, Baltimore, USA, June 8-10, 2004.

[8] A. Taghizad, J. Jimenez, L. Binet, D. Heuze, "*Experimental and theoretical investigations to develop a model of rotor aerodynamics adapted to steep descents*", AHS International, 58th Annual Forum Proceedings, Montreal, Canada, vol. 1, pp. 613-626, June 2002.

[9] J. Leishman, M. Bagwat, S. Ananthan, *"The Vortex Ring State as a spatially and temporally developing wake instabilities"*, Proceedings the American Helicopter Society annual forum, Jan. 2002.

[10] S. Newman, R. Brown, *"Predicting the onset of wake breakdown for rotors in descending flight"*, Journal of American Helicopter Society

[11] E. Hoindville, T. Renaud, *"CFD simulation of helicopter rotor in the Vortex Ring State regime"*, American Helicopter Society 63rd annual forum, Virginia Beach, VA, May 1-3, 2007.

[12] B. Benoit, A-M. Dequin, K. Kampa, W. Grunhagen, P-M. Basset, *"HOST: a General Helicopter Tool for Germany and France"*, 56th Annual Forum of the American Helicopter Society, Virginia Beach, May 2000.

[13] J. Jimenez, A. Desopper, A. Taghizad, L. Binet, *"Induced velocity model in steep descent and vortex-ring state prediction"*, 27th European Rotorcraft Forum, Moscow, Russia; 11-14 Sept. 2001

[14] S. Muller, A. Leroy, P. Devinant, *"An Unsteady Lifting Line Approach for Curved and Swept Wings Aerodynamic Computation"*, 13th International Conference on Fluid Flow Technologies, Budapest, Hungary, Sept. 6-9, 2006